PUBLICATIONS OF THE ASTRONOMICAL SOCIETY OF THE PACIFIC, **118**: 733–739, 2006 May

SDSS Preburst Observations of Recent Gamma-Ray Burst Fields

RICHARD J. COOL,[1] DANIEL J. EISENSTEIN,[1] DAVID W. HOGG,[2] MICHAEL R. BLANTON,[2] DAVID J. SCHLEGEL,[3]
J. BRINKMANN,[4] DONALD P. SCHNEIDER,[5] AND DANIEL E. VANDEN BERK[5]
Received 2006 January 10; accepted 2006 February 13; published 2006 May 23

ABSTRACT. We present Sloan Digital Sky Survey (SDSS) photometry and spectroscopy in the fields of 27 gamma-ray bursts observed by *Swift*, including bursts localized by *Swift*, *HETE-2*, and *INTEGRAL*, after 2004 December. After this bulk release, we plan to provide individual releases of similar data shortly after the localization of future bursts falling in the SDSS survey area. These data provide a solid basis for the astrometric and photometric calibration of follow-up afterglow searches and monitoring. Furthermore, the images provided with this release will allow observers to find transient objects up to a magnitude fainter than is possible with Digitized Sky Survey images.

1. INTRODUCTION

Prompt long-wavelength follow-up observations of gamma-ray bursts (GRBs) have revolutionized the study of these energetic and enigmatic objects. With the successful launch of recent high-energy missions such as the *High Energy Transient Explorer 2* (*HETE-2*; Lamb et al. 2004), the *International Gamma-Ray Astrophysics Laboratory* (*INTEGRAL*; Winkler et al. 2003), and *Swift* (Gehrels et al. 2004), rapid follow-up of gamma-ray bursts has come to maturity. *Swift* and *HETE-2* not only detect new GRBs, but also provide rapid X-ray localization that allows for very precise positions (with uncertainties as small as a few arcseconds), far superior than was previously possible. Modern GRB samples have become large enough to study the statistical properties of GRBs (e.g., Berger et al. 2005c), and rapid follow-up observations have allowed for the first optical, radio, and X-ray localization of afterglows from short-hard gamma-ray bursts (Gehrels et al. 2005; Hjorth et al. 2005; Villasenor et al. 2005; Fox et al. 2005; Pedersen et al. 2005; Prochaska et al. 2006; Covino et al. 2006; Berger et al. 2005b; Bloom et al. 2006).

There has been large-scale success in identifying afterglows and conducting prompt spectroscopic follow-up; afterglows extending out to $z \sim 6.3$ (Price et al. 2005; Kawai et al. 2005) have been spectroscopically confirmed, providing luminous probes of the universe as far back as the era of reionization. Recently, high-resolution spectroscopy of GRBs has allowed for detailed studies of absorbing systems arising in the local environment of the GRB progenitor (Berger et al. 2006; Chen et al. 2005). Absorption-line analyses of GRB afterglow spectra show structure similar to that of quasar damped Lyα absorbers (DLAs) but extending to higher hydrogen column densities and including several metal lines not found in quasar DLA systems (Watson et al. 2006; Chen et al. 2005).

It has been suggested that GRBs can provide a new class of standard candle for future cosmological experiments (Ghirlanda et al. 2004a, 2004b; Friedman & Bloom 2005; Bloom et al. 2003). As the luminosities of these objects should allow detection to very high redshifts ($z > 10$; Lamb & Reichart 2000), studies of GRBs could extend current work using Type Ia supernovae to high redshifts, thus providing considerable constraints on our understanding of cosmology. Before gamma-ray bursts can be used as a cosmological tool, however, a large number of bursts must be observed spectroscopically in order to calibrate the method.

Two keys to studying GRB afterglows are the identification of a transient afterglow coincident with the burst detected at high energies, and high-quality information for in-field photometric calibration stars so that all observations can be placed onto a common photometric system. Currently, many afterglow searches compare new data to digitized Palomar Observatory Sky Survey photometric plates (DSS [Digitized Sky Survey]) and use US Naval Observatory (USNO) stars (Monet et al. 1998) to calibrate both astrometry and photometry. As larger telescopes join the search for afterglows, the DSS imaging quickly becomes insufficient, because these images are too shallow to make detailed comparisons to deep optical imaging; therefore, afterglow candidates can only be identified through their temporal properties. The USNO catalog is an astrometric catalog, but it was not intended to be a source of photometric calibration across the sky; USNO-calibrated photometry may

[1] Steward Observatory, University of Arizona, 933 North Cherry Avenue, Tucson, AZ 85721; rcool@as.arizona.edu.
[2] Department of Physics, Center for Cosmology and Particle Physics, 4 Washington Place, New York University, New York, NY 10003.
[3] Lawrence Berkeley National Laboratory, 1 Cyclotron Road, Mail Stop 50R232, Berkeley, CA 94720.
[4] Apache Point Observatory, 2001 Apache Point Road, Sunspot, NM 88349.
[5] Department of Astronomy and Astrophysics, Pennsylvania State University, 525 Davey Laboratory, University Park, PA 16802.

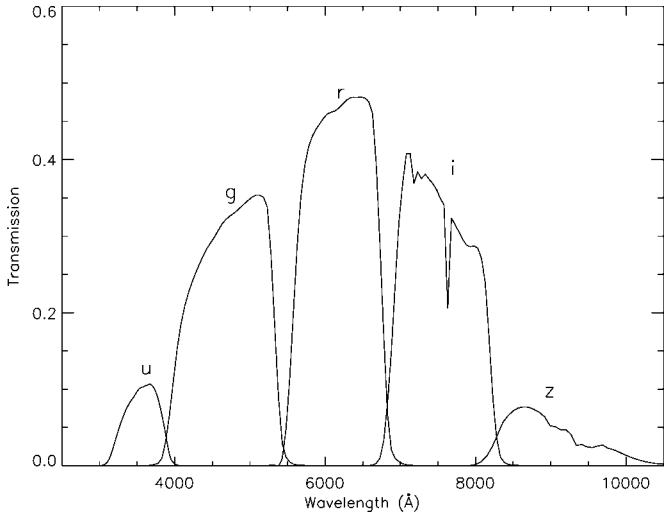

FIG. 1.—Transmission curves for the standard SDSS *ugriz* photometric system. Each of the response curves assumes an air mass of 1.3 and includes the quantum efficiency of the CCD camera and the reflectivity of the primary and secondary mirrors on the SDSS telescope.

thus be strongly affected by systematic photometric residuals in the USNO catalog itself.

The Sloan Digital Sky Survey (SDSS; York et al. 2000) provides accurate photometry and astrometry for objects over one-quarter of the sky, making it a viable alternative to the DSS images and USNO catalogs. The imaging from the SDSS extends over a magnitude deeper than that of the DSS, making it a valuable resource for identifying transient objects, while the stable photometric and astrometric calibration of the survey makes it an ideal source of calibration data in GRB fields. In order to aid the community, we are releasing SDSS imaging and spectroscopy for the fields of 27 *Swift*-observed GRBs detected after 2004 December, including bursts originally localized by *Swift*, *HETE-2*, and *INTEGRAL* observations. Here we offer a bulk release of GRB fields observed in the SDSS, but in the future, we will release similar data through the GRB Coordinates Network (GCN) shortly after the detection of a new burst within the SDSS survey area.

In this paper, we provide some basic documentation relating to the Sloan Digital Sky Survey and describe the data products included in each GRB release. We hope that the information provided here will be a useful primer for those who are unfamiliar with SDSS data; however, this document is by no means intended to be a full description of the survey or survey data products. The layout of the paper is as follows. In § 2, we describe the Sloan Digital Sky Survey itself. A brief description of photometric quantities measured in the SDSS is given in § 3. We describe the data products provided with each GRB release in § 4 and offer some concluding remarks in § 5.

TABLE 1
EFFECTIVE WAVELENGTHS OF SDSS BANDPASSES

Filter	*u*	*g*	*r*	*i*	*z*
$\lambda_{\rm eff}$ (Å) ……	3546	4670	6156	7472	8917

2. THE SLOAN DIGITAL SKY SURVEY

The Sloan Digital Sky Survey (York et al. 2000; Stoughton et al. 2002a; Abazajian et al. 2003, 2004, 2005; Adelman-McCarthy et al. 2006) is imaging π steradians of the sky through five filters, *ugriz* (Fukugita et al. 1996; see Fig. 1 and Table 1 for transmission curves and effective wavelengths). The imaging is conducted with a CCD mosaic in drift-scanning mode (Gunn et al. 1998) on a dedicated 2.5 m telescope (Gunn et al. 2006) located at Apache Point Observatory in New Mexico. Images are processed (Lupton et al. 2001; Stoughton et al. 2002b; Pier et al. 2003; Lupton 2006) and calibrated (Hogg et al. 2001; Smith et al. 2002; Ivezić et al. 2004; Tucker et al. 2006), after which targets are selected for spectroscopy (Eisenstein et al. 2001; Strauss et al. 2002; Richards et al. 2002) with two double spectrographs that are mounted on the same telescope and use a fiber allocation algorithm that ensures highly complete spectroscopic samples (Blanton et al. 2003). The reduced spectra are classified, and redshifts are determined using the `idlspec2d` automated pipeline (D. Schlegel et al. 2006, in preparation).

The photometric calibration of SDSS imaging results in photometry that is nearly on an AB system (Oke 1974). The details of SDSS photometric calibration are beyond the scope of this document (the interested reader can find the calibration procedure in the data-release papers and technical papers cited above); the bottom line is that the photometric calibration in the SDSS is quite robust, with small random errors. When considering the position of the bright-star stellar locus in color-color space, the rms errors are found to be 0.01 mag in the *g*, *r*, and *i* bandpasses, 0.02 mag in the *z* band, and 0.03 in the *u* band (Ivezić et al. 2004). Similarly small photometric errors have been demonstrated by measuring the small scatter in the colors of early-type galaxies on the red sequence (Cool et al. 2006). It should be noted that the data provided in these preburst GRB releases have been processed using a slightly different pipeline than that used for the SDSS public data releases. We cannot guarantee that the values presented here will exactly match those from the SDSS public data releases; in particular, we expect the photometric calibrations to differ on the order of 0.01 mag.

Astrometric calibration within the SDSS is also quite robust. Relative astrometry is generally better than 50 mas per coordinate, while the absolute astrometry is generally better than 0.″1 per coordinate (Pier et al. 2003). It should be noted that the SDSS astrometric system can have systematic offsets with respect to other astrometric catalogs. Users requiring high-accuracy astrometry should check for any such offsets when

making comparisons between SDSS astrometry and data calibrated to another astrometric system.

Users of $UBVR_CI_C$ imaging may also find the transformations (both empirically measured and theoretically derived) between the $UBVR_CI_C$ and *ugriz* photometric systems described in Fukugita et al. (1996) and Smith et al. (2002) to be useful when using the photometry included in our GRB releases to calibrate new observations.

3. MEASURED QUANTITIES

In this section, we outline the definitions of several of the photometric measurements that are used in the SDSS and are included in this data release. This description is by no means an exhaustive source of information. Much more detailed descriptions of the SDSS data products can be found in the data-release papers and the technical papers referenced in the previous section.

3.1. SDSS Magnitudes and Fluxes

All SDSS magnitudes, including those presented in this and future GRB releases, are expressed in terms of asinh magnitudes (Lupton et al. 1999). At high signal-to-noise ratios (S/Ns), asinh magnitudes are identical to the standard logarithmic magnitude (Pogson 1856). However, asinh magnitudes are well behaved even at very low or even negative fluxes, allowing for magnitude calculations even without a formal object detection. As described in Stoughton et al. (2002a), the asinh magnitude for a measured flux f is given by

$$m = -\frac{2.5}{\ln 10}\left[\operatorname{asinh}\left(\frac{f/f_0}{2b}\right) + \ln b\right]. \quad (1)$$

Here f_0 defines the zero point of the magnitude scale, and the softening parameter b denotes the typical 1 σ noise of the sky in a point-spread function (PSF) aperture in 1″ seeing. Table 2, which is a reproduction of Table 21 in Stoughton et al. (2002a), lists the values of b and the magnitude corresponding to a zero-flux measurement. The table further lists m_c, corresponding to a flux of $10f_0b$; asinh and logarithmic magnitudes differ by less than 1% in flux for objects brighter than this limit.

In this and future preburst data releases, we report photometry in flux units and in magnitudes. All flux measurements presented in these releases have units of nanomaggies. A nanomaggie is a flux-density unit equal to 10^{-9} of a magnitude zero source. As SDSS is nearly an AB system, 1 nanomaggie corresponds to 3.631 μJy, or 3.631×10^{-29} ergs s^{-1} cm^{-2} Hz^{-1}.

3.2. PSF Magnitudes

For each object detected in the SDSS imaging, a locally determined model of the point-spread function (PSF) is used to measure the flux contained within a PSF centered on the location of the source. An aperture correction is applied to each frame, based on both the local PSF model and the seeing in the frame. Details on these aperture corrections are given in Stoughton et al. (2002a). The errors reported for the PSF fluxes include contributions from counting statistics as well as uncertainties in the aperture corrections and PSF modeling. PSF magnitudes are the preferred photometric measurement for point-sources such as stars and quasars.

TABLE 2
asinh MAGNITUDE PARAMETERS

Filter	b	Zero-Flux Magnitude	m_c
u	1.4×10^{-10}	24.63	22.12
g	0.9×10^{-10}	25.11	22.60
r	1.2×10^{-10}	24.80	22.29
i	1.8×10^{-10}	24.36	21.85
z	7.4×10^{-10}	22.83	20.32

3.3. Model Magnitudes

Two galaxy models are fit to the two-dimensional image of each object detected in the SDSS, a pure de Vaucouleurs profile,

$$I(r) = I_0 \exp\left[-7.67(r/r_e)^{1/4}\right] \quad (2)$$

(de Vaucouleurs 1948) and a pure exponential profile,

$$I(r) = I_0 \exp\left(-1.68r/r_e\right). \quad (3)$$

Each of the models is convolved with the local PSF before fitting to the image. The best-fit model is chosen in the r band; this is the model used to calculate the model quantities for the object. In order to provide meaningful colors, the photometric pipeline fits the full profile in the r-band image, and the images from the other bands are fitted such that only the amplitude of the profile is allowed to vary (Stoughton et al. 2002a). In the absence of color gradients, model colors provide an unbiased measurement of galaxy colors.

3.4. Petrosian Magnitudes

The Petrosian ratio $\mathcal{R}_P$ (Petrosian 1976), the ratio of the local surface brightness at radius θ to the average surface brightness at that radius, is given by

$$\mathcal{R}_P(\theta) \equiv \frac{\int_{\alpha_{lo}\theta}^{\alpha_{hi}\theta} d\theta'\, 2\pi\theta' I(\theta')/[\pi(\alpha_{hi}^2 - \alpha_{lo}^2)\theta^2]}{\int_0^{\theta} dr'\, 2\pi\theta' I(\theta')/(\pi\theta^2)}, \quad (4)$$

where $I(\theta)$ is the azimuthally averaged surface brightness profile of a galaxy and α_{lo} and α_{hi} are chosen to be 0.85 and 1.25 for SDSS. The Petrosian flux is given by the flux within a circular aperture of $2\theta_P$, where θ_P is the radius at which $\mathcal{R}_P$ falls below 0.2. In the SDSS, θ_P is determined in the r band and is sub-

TABLE 3
QUANTITIES LISTED IN sdss.calstar FILES

File Column	Description
1	Right ascension (J2000.0)
2	Declination (J2000.0)
3–7	*ugriz* PSF magnitudes
8–12	*ugriz* PSF magnitude errors
9–13	Quality flags in each filter

sequently used in each of the other bands. In the absence of seeing effects, this flux measurement contains a constant fraction of a galaxy's light, independent of its size or distance, and thus provides a fair flux measurement when comparing galaxies of different sizes or at different redshifts. More details on SDSS Petrosian magnitudes can be found in Blanton et al. (2001), Strauss et al. (2002), and Stoughton et al. (2002a).

3.5. Flags

A number of data quality flags are maintained in order to guarantee the accuracy of photometric measurements in the SDSS. A full description of these flags is beyond the scope of this document but can be found in the Early Data Release paper (Stoughton et al. 2002a) and at the SDSS DR4 Web site.[6] For each object included in this release, we provide five quality flags (one for each band) based on the flags output by the SDSS pipeline. In brief, we collapse all of the SDSS data quality flags into a single "yes" or "no" quality indicator. Data that are marked as suspect (flag = 1) should be used with caution.

4. DATA PRODUCTS

In this section, we describe each of the data products provided in this data release. We have removed saturated stars from all of the data tables and have *not* corrected the photometry for Galactic extinction. Again, magnitudes are asinh magnitudes, as is standard in the SDSS.

4.1. sdss.calstar

For each burst, we report the photometry and astrometry of bright stars ($r < 20.5$) within 15′ of the burst location, in files labeled sdss.calstar. These stars provide a reliable basis for both the astrometric and photometric calibration of GRB follow-up imaging. The area covered by these calibration stars is well matched to the *Swift* X-Ray Telescope field of view (Gehrels et al. 2004). Table 3 lists the information provided for each of the calibrations stars in the sdss.calstar file for each GRB data set. It is important that the user consult the object flags and photometric errors when utilizing stars from this file, as some of the stars are poorly detected in the *u* band.

[6] See http://www.sdss.org/dr4/products/catalogs/flags.html.

TABLE 4
QUANTITIES LISTED IN sdss.objects FILES

File Column	Description
1	Right ascension (J2000.0)
2	Declination (J2000.0)
3	Object type: star = 6 galaxy = 3
4–8	*ugriz* model magnitudes
9–13	*ugriz* model magnitude errors
14–18	*ugriz* Petrosian magnitudes
19–23	*ugriz* Petrosian magnitude errors
24–28	Quality flags in each filter

4.2. sdss.objects

In the sdss.objects_flux and sdss.objects_magnitudes files, we provide photometry and astrometry of all unsaturated objects with $r < 23.0$ within 6′ of the GRB location. As suggested by the file names, photometric quantities in the sdss.objects_flux file use flux units (nanomaggies), while those in the sdss.objects_magnitudes file use magnitudes (asinh magnitudes). Table 4 lists the quantities reported in these files.

We recommend using model fluxes when calculating colors of galaxies with $r > 19.0$. We generally prefer Petrosian fluxes over model fluxes for the overall flux of a galaxy, but Petrosian fluxes are noisier than model quantities at faint flux levels. We warn the user to exercise caution when using photometry with quoted flux errors larger than 20%. These objects are generally only low-S/N detections, but sometimes the large errors indicate complications in the reductions.

4.3. sdss.spectro

If SDSS spectroscopy has been completed in the field of the GRB, the sdss.spectro file will include redshifts of spectroscopically observed objects within 6′ of the GRB location. Table 5 documents the parameters reported in the sdss.spectro files. For stars and galaxies, redshifts are accurate to approximately 30 km s^{-1}, while quasar redshifts, which are of less importance here, are measured to $\Delta z = 0.001$ (Stoughton et al. 2002a). All redshifts have been corrected to a heliocentric frame but are not corrected for Galactic rotation.

TABLE 5
QUANTITIES LISTED IN sdss.spectro FILES

File Column	Description
1	Right ascension (J2000.0)
2	Declination (J2000.0)
3	Spectroscopic classification
4	Spectroscopic subclass
5	Measured redshift
6	1 σ error on redshift
7	SDSS spectroscopic plate
8	SDSS spectroscopic fiber
9	MJD of SDSS spectroscopic observation

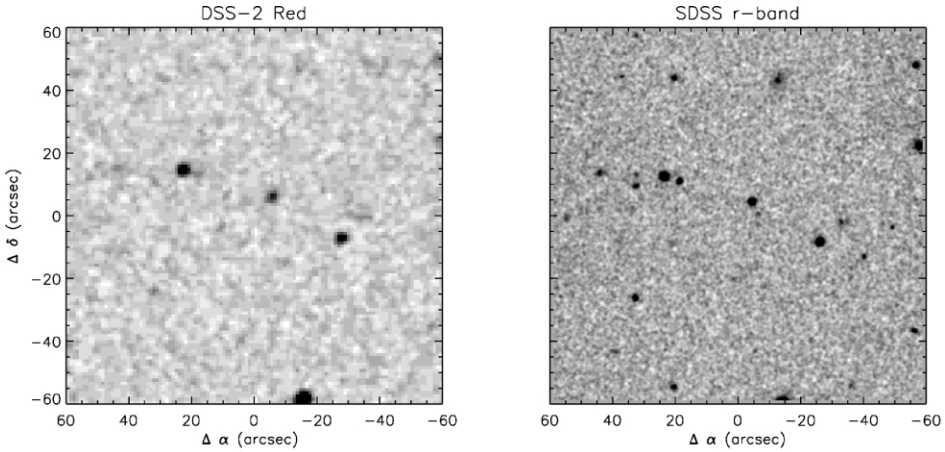

FIG. 2.—Comparison of the DSS-2 red and SDSS imaging for a 1′ × 1′ box around the location of *Swift* GRB 041224. The *Swift* BAT localization (Barthelmy et al. 2004) is at the origin in both images. The SDSS image clearly extends deeper than the DSS-2 image, making it a more valuable comparison epoch when searching for GRB afterglows.

Each spectroscopically observed object is classified by a spectral class (STAR, GALAXY, or QSO) and a spectral subclass if appropriate. Galaxies can be subclassified as STARFORMING, AGN, or STARBURST, depending on the strength of the emission lines observed in the spectrum. Both galaxies and quasars can be subclassified as BROADLINE, based on the width of the emission-line features; stars are subclassified by spectral type.

4.4. Images

For an 8′ × 8′ region around each burst, we include gzipped FITS images in each of the SDSS passbands, as well as three-color composite (*gri*) images of the field in JPEG format. The FITS images are in units of nanomaggies per pixel, where a pixel is 0.″396 on a side. Each of the images is oriented with north up and east to the left, and the FITS headers include the relevant World Coordinate System information. The SDSS images provide an important comparison epoch for follow-up imaging in order to locate possible gamma-ray burst afterglows. To illustrate the power of using SDSS images compared to those from the Digitized Sky Survey, Figure 2 shows a 1′ × 1′ region around the field of GRB 041224 as imaged in SDSS and the DSS-2 red plates. Both images are centered on the position of the GRB as reported by the *Swift* Burst Alert Telescope (BAT) detection (Barthelmy et al. 2004). The imaging from the SDSS reaches over a magnitude deeper than the DSS imaging, allowing for the identification of transient objects to fainter limits than are possible using the DSS.

5. DATA RELEASE AND APPLICATION

In this paper, we present SDSS observations of all *Swift*-observed gamma-ray bursts occurring after 2004 December that lie in the SDSS imaging footprint. For convenience, we include not only data for burst fields with photometry included in previous SDSS data releases, but also bursts for which the data have not yet been released by the SDSS. Table 6 lists the bursts included in this release, in addition to the current status of the data and the number of calibration stars, surrounding objects, and spectroscopically observed objects located in each GRB field.

All of the data included in this release, as well as data we will release in the future, can be found on the online SDSS GRB release page.[7] In addition to all of the data products described in the previous section, we also include a short text file for each burst. This short description provides a brief introduction to the data products and reports the local mean galactic extinction for each GRB field. In the future, we will release SDSS imaging and spectroscopy of individual GRB fields shortly after the bursts are localized. These future data releases will be announced via a GCN Circular and, unless otherwise noted, follow the same data release model described in this document. All data from this release and future preburst data releases may be used freely, but we request that both the most recent SDSS data release paper (currently Adelman-McCarthy et al. 2006) and this paper (for bursts included in the current release) or the GCN Circular (for bursts released in the future) be cited.

6. ACKNOWLEDGMENTS

R. J. C. is funded through a National Science Foundation Graduate Student Fellowship. This research has made use of NASA's Astrophysics Data System bibliographic services. The Second Palomar Observatory Sky Survey (POSS-II) was made by the California Institute of Technology with funds from the

[7] See http://mizar.as.arizona.edu/grb/public.

TABLE 6
GRBs Covered in This Release

GRB	α (J2000.0) (deg)	δ (J2000.0) (deg)	N_{cal}	N_{obj}	N_{spec}	Position GCN	SDSS Status
041224	56.200	−6.620	280	791	12	2908	Public
050124	192.877	13.044	338	688	4	2974	Public
050215B	174.449	40.796	167	463	5	3027	Private
050319	154.200	43.548	238	476	2	3133	Private
050408	180.573	10.852	231	593	6	3191	Private
050412	181.105	−1.201	274	450	2	3241	Private
050416A	188.478	21.057	232	596	0	3268	Public
050504	201.005	40.703	192	654	1	3359	Private
050505	141.763	30.273	286	832	2	3365	Private
050509B	189.058	28.984	118	976	0	3381	Public
050520	192.526	30.451	229	858	0	3434	Public
050522	200.081	24.770	132	769	0	3452	Public
050528	353.529	45.944	2019	988	3	3496	Public
050715	155.645	−0.040	392	958	6	3621	Private
050802	219.275	27.786	417	622	0	3734	Private
050813	241.988	11.248	840	774	0	3788	Public
050819	358.756	24.859	598	1140	0	3826	Public
050904	13.711	14.085	412	638	5	3910	Public
050922C	317.389	−8.758	663	774	0	4013	Public
051008	202.872	42.100	257	408	4	4071	Private
051114	226.267	60.156	222	282	1	4279	Private
051117A	228.391	30.870	399	541	4	4287	Private
051215	163.139	38.626	162	1112	8	4352	Private
051227	125.270	31.929	552	1294	4	4397	Public
060108	147.006	31.918	187	630	2	4444	Public
060121	137.488	45.675	301	507	3	4550	Public
060123	179.700	45.513	166	376	1	4584	Private

National Science Foundation, the National Aeronautics and Space Administration, the National Geographic Society, the Sloan Foundation, the Samuel Oschin Foundation, and the Eastman Kodak Corporation.

Funding for the SDSS and SDSS-II has been provided by the Alfred P. Sloan Foundation, the Participating Institutions, the National Science Foundation, the US Department of Energy, the NASA, the Japanese Monbukagakusho, the Max Planck Society, and the Higher Education Funding Council for England. The SDSS Web Site is http://www.sdss.org.

The SDSS is managed by the Astrophysical Research Consortium for the Participating Institutions. The Participating Institutions are the American Museum of Natural History, Astrophysical Institute Potsdam, University of Basel, Cambridge University, Case Western Reserve University, University of Chicago, Drexel University, Fermilab, the Institute for Advanced Study, the Japan Participation Group, Johns Hopkins University, the Joint Institute for Nuclear Astrophysics, the Kavli Institute for Particle Astrophysics and Cosmology, the Korean Scientist Group, the Chinese Academy of Sciences (LAMOST), Los Alamos National Laboratory, the Max-Planck-Institute for Astronomy (MPA), the Max-Planck-Institute for Astrophysics (MPIA), New Mexico State University, Ohio State University, University of Pittsburgh, University of Portsmouth, Princeton University, the United States Naval Observatory, and the University of Washington.

REFERENCES

Abazajian, K., et al. 2003, AJ, 126, 2081
———. 2004, AJ, 128, 502
———. 2005, AJ, 129, 1755
Adelman-McCarthy, J. K., et al. 2006, ApJS, 162, 38
Barthelmy, S., et al. 2004, GCN Circ. 2908
Berger, E., Penprase, B. E., Cenko, S. B., Kulkarni, S. R., Fox, D. B., Steidel, C. C., & Reddy, N. A. 2006, ApJ, 642, 979
Berger, E., et al. 2005b, Nature, 438, 988
Berger, E., et al. 2005c, ApJ, 634, 501
Blanton, M. R., Lin, H., Lupton, R. H., Maley, F. M., Young, N., Zehavi, I., & Loveday, J. 2003, AJ, 125, 2276
Blanton, M. R., et al. 2001, AJ, 121, 2358
Bloom, J. S., Frail, D. A., & Kulkarni, S. R. 2003, ApJ, 594, 674
Bloom, J. S., et al. 2006, ApJ, 638, 354
Chen, H.-W., Prochaska, J. X., Bloom, J. S., & Thompson, I. B. 2005, ApJ, 634, L25
Cool, R. J., Eisenstein, D. J., Johnston, D., Scranton, R., Brinkmann, J., Schneider, D. P., & Zehavi, I. 2006, AJ, 131, 736
Covino, S., et al. 2006, A&A, 447, 5
de Vaucouleurs, G. 1948, Ann. d'Astrophys., 11, 247
Eisenstein, D. J., et al. 2001, AJ, 122, 2267
Fox, D. B., et al. 2005, Nature, 437, 845
Friedman, A. S., & Bloom, J. S. 2005, ApJ, 627, 1

Fukugita, M., Ichikawa, T., Gunn, J. E., Doi, M., Shimasaku, K., & Schneider, D. P. 1996, AJ, 111, 1748
Gehrels, N., et al. 2004, ApJ, 611, 1005
———. 2005, Nature, 437, 851
Ghirlanda, G., Ghisellini, G., & Lazzati, D. 2004a, ApJ, 616, 331
Ghirlanda, G., Ghisellini, G., Lazzati, D., & Firmani, C. 2004b, ApJ, 613, L13
Gunn, J. E., et al. 1998, AJ, 116, 3040
———. 2006, AJ, 131, 2332
Hjorth, J., et al. 2005, Nature, 437, 859
Hogg, D. W., Finkbeiner, D. P., Schlegel, D. J., & Gunn, J. E. 2001, AJ, 122, 2129
Ivezić, Ž., et al. 2004, Astron. Nachr., 325, 583
Kawai, N., et al. 2005, Nature, 440, 184
Lamb, D. Q., & Reichart, D. E. 2000, ApJ, 536, 1
Lamb, D. Q., et al. 2004, Nucl. Phys. B Proc. Suppl., 132, 279
Lupton, R. H. 2006, AJ, submitted
Lupton, R. H., Gunn, J. E., Ivezić, Z., Knapp, G. R., Kent, S., & Yasuda, N. 2001, in ASP Conf. Ser. 238, Astronomical Data Analysis Software and Systems X, ed. F. R. Harnden, Jr., F. A. Primini, & H. E. Payne (San Francisco: ASP), 269
Lupton, R. H., Gunn, J. E., & Szalay, A. S. 1999, AJ, 118, 1406
Monet, D. B. A., et al. 1998, USNO-A V2.0, A Catalog of Astrometric Standards (Flagstaff: USNO)
Oke, J. B. 1974, ApJS, 27, 21
Pedersen, K., et al. 2005, ApJ, 634, L17
Petrosian, V. 1976, ApJ, 209, L1
Pier, J. R., Munn, J. A., Hindsley, R. B., Hennessy, G. S., Kent, S. M., Lupton, R. H., & Ivezić, Ž. 2003, AJ, 125, 1559
Pogson, N. 1856, MNRAS, 17, 12
Price, P. A., Cowie, L. L., Minezaki, T., Schmidt,. P., Songaila, A., & Yoshii, Y. 2005, ApJ, in press (astro-ph/0509697)
Prochaska, J. X., et al. 2006, ApJ, 642, 989
Richards, G. T., et al. 2002, AJ, 123, 2945
Smith, J. A., et al. 2002, AJ, 123, 2121
Stoughton, C., et al. 2002a, AJ, 123, 485
———. 2002b, Proc. SPIE, 836, 339
Strauss, M. A., et al. 2002, AJ, 124, 1810
Tucker, D., et al. 2006, AJ, submitted
Villasenor, J. S., et al. 2005, Nature, 437, 855
Watson, D., et al. 2006, ApJ, submitted (astro-ph/0510368)
Winkler, C., et al. 2003, A&A, 411, L1
York, D. G., et al. 2000, AJ, 120, 1579